THE UNIVERSITY OF READING

USE OF A DISCRETE NORM IN BEST PIECEWISE CONSTANT APPROXIMATION OF CONTINUOUS FUNCTIONS ON IRREGULAR GRIDS

by

M J Baines

Numerical Analysis Report 6/95

DEPARTMENT OF MATHEMATICS

The University of Reading

Use of a Discrete Norm in Best Piecewise Constant Approximation of Continuous Functions on Irregular Grids

by

M J Baines

Numerical analysis report 6/95

Department of Mathematics
P O Box 220
Reading RG6 2AF

Abstract

This report describes an algorithm for generating "optimal" grids for the representation of continuous functions by piecewise constant approximation in one and two dimensions on unstructured grids, using a discrete norm. The algorithm incorporates a convergent iteration, each step of which reduces the norm. The approach provides a link with heuristic averaging procedures used in grid adaptation, providing a rationale for their use. The extension to three dimensions is straightforward.

Introduction

The purpose of this report is twofold. First, it presents a simple way of constructing an optimal mesh for the piecewise constant approximation of a continuous function in a simple discrete norm, both in one and two dimensions on an unstructured grid. The more complicated L_2 case was discussed in [1] and analysed in [2]. The algorithms presented here shares with [1] the property that it produces a mesh sequence for which the error norm converges.

The second purpose is to bring out the similarities between this algorithm and an heuristic averaging procedure used in grid generation. This gives a rationale for the averaging procedure and a simple interpretation of the algorithm for the best fit.

One of the disadvantages of the algorithms for best constant fits using the L_2 norm described in [1] is the complexity of solving the equation for the grid iteration step. Here we replace the L_2 norm by a discrete norm which enables a simple formula to be derived while preserving the norm-reducing property of the method. The discrete norm is almost equivalent to a trapezium rule quadrature version of the L_2 norm approach given in [1] but the size of the element is omitted. Its inclusion considerably alters the variation of the norm under grid movement and is the source of the complications seen in [1].

In section 2 the discrete norm is introduced in one dimension and an algorithm proposed which reduces the norm of the error at every step of an iteration in which the grid adapts. The algorithm therefore converges in the sense that the norm of the error tends to a limit, although the grid itself may not (as discussed in [2]) tend to a global minimum.

A weight function may be included in the norm but for norm reduction the theory restricts it to be independent of the data function. If this restriction is violated the norm reduction property cannot be proved, but the algorithm may nevertheless continue to work in practice. A particular feature of the algorithm is the similarity between the grid movement step and certain averaging procedures used in grid adaptation methods.

In section 3 the procedure is extended to two dimensions. The same property of norm reduction is proved, so that once again a limit exists. Also averaging procedures familiar in grid adaptation once again involved, particularly when the weight function is allowed to depend on the function, and this similarity is brought out in section 4.

Section 5 concerns generalisations of the ideas, including the extension to 3-D. Several demonstrations of the results of the algorithm are presented in section 6. Finally, in section 7 we summarise the report and present some ideas for future developement and use.

2. One Dimension

2.1 A Discrete Norm

Let $f \in C[0,1]$ be a given continuous function. For a given integer N, let T^N be the set of all partitions $\tilde{\Pi}$ of $[0,1]$ with N interior points, i.e.

$$\tilde{\Pi}: \; 0 = x_0 < x_1 < \ldots < x_N < x_{N+1} = 1.$$

For a given $\tilde{\Pi}$ define

$$D(\tilde{\Pi}) = \left\{ v \in L^2[0,1] \middle| v|_{[x_{j-1},x_j]} = \text{ constant, for } j = 1,\ldots,N+1 \right\}.$$

Now introduce the discrete norm $\|\cdot\|$ with positive weight w given by

$$\|g\|^2 = \sum_{k=1}^{N+1} w_k \{g(x_{kL})^2 + g(x_{kR})^2\} \tag{2.1}$$

(see Fig. 1a), where the suffices L and R refer to the left and right hand ends of the interval. We seek the element $u \in D(\Pi)$ and the partition Π such that

$$\|u - f\| \leq \|v - f\| \text{ for all } v \in D(\Pi) \text{ and } \Pi \in \mathrm{T}^N.$$

Given the partition Π, the projection of u of f in the norm (2.1) is defined as the unique element of $D(\Pi)$ such that

$$\|u - f\| \leq \|v - f\| \text{ for all } v \in D(\Pi) \;. \tag{2.2}$$

From (2.1), written in the form

$$\|g\|^2 = \tfrac{1}{2} \sum_{k=1}^{N+1} w_k \{(g(x_{kL}) + g(x_{kR}))^2 + (g(x_{kL}) - g(x_{kR}))^2\}, \tag{2.3}$$

it is easy to verify that

$$\|v-f\|^2 = \tfrac{1}{2}\sum_{k=1}^{N+1} w_k\{(v_k - f(x_{kL}) + v_k - f(x_{kR}))^2 + (f(x_{kL}) - f(x_{kR}))^2\} \quad (2.4)$$

is minimised by the element u for which

$$u_k = \tfrac{1}{2}\{f(x_{kL}) + f(x_{kR})\}. \quad (2.5)$$

Now seek the partition $\Pi \in \mathrm{T}^N$ with corresponding projection

$u = u(\Pi) \in D(\Pi)$ such that

$$\|u(\Pi) - f\| \le \|u(\tilde{\Pi}) - f\| \quad \text{for all } \tilde{\Pi} \in \mathrm{T}^N. \quad (2.6)$$

First write (2.1) as

$$\|g\|^2 = w_j^+(g_0^+)^2 + \sum_{j=1}^{N}\{w_j^-(g_j^-)^2 + w_j^+(g_j^+)^2\} + w_{N+1}^-(g_{N+1}^-)^2 \quad (2.7)$$

where

$$w_j^- = w_{j-\frac{1}{2}}, \quad g_j^- = g\big|_{[x_{j-1},x_j]}$$

$$w_j^+ = w_{j+\frac{1}{2}}, \quad g_j^+ = g\big|_{[x_j,x_{j+1}]}$$

(see Fig. 1b). Using the identity

$$w_j^-(g_j^-)^2 + w_j^+(g_j^+)^2 = \{(w_j^- g_j^- + w_j^+ g_j^+)^2 + w_j^- w_j^+ (g_j^- - g_j^+)^2\}/(w_j^- + w_j^+) \quad (2.8)$$

(2.7) becomes

$$\|g\|^2 = w_0^+(g_0^+)^2 + \sum_{j=1}^{N}\frac{\{(w_j^- g_j^- + w_j^+ g_j^+)^2 + w_j^- w_j^+(g_j^- - g_j^+)^2\}}{w_j^- + w_j^+} + w_{N+1}^-(g_{N+1}^-)^2. \quad (2.9)$$

Then

$$\|u-f\|^2 = w_0^+(u_0^+ - f(x_0))^2 + \sum_{j=1}^{N}\frac{\{(w_j^-(u_j^- - f(x_j)) + w_j^+(u_j^+ - f(x_j))\}^2}{w_j^- + w_j^+}$$

$$+\sum_{j=1}^{N}\frac{w_j^- w_j^+}{w_j^- + w_j^+}(u_j^- - u_j^+)^2 + w_{N+1}^-(u_{N+1}^- - f(x_{N+1}))^2 \tag{2.10}$$

which is minimised, for a given piecewise constant function u, by the partition Π with interior points $x_j (j = 1,2,\ldots,N)$ such that

$$w_j^-(u_j^- - f(x_j)) + w_j^+(u_j^+ - f(x_j)) = 0 \tag{2.11}$$

or

$$f(x_j) = \frac{w_j^- u_j^- + w_j^+ u_j^+}{w_j^- + w_j^+} = \bar{u}_j, \quad \text{say}. \tag{2.12}$$

Since the right hand side of (2.12) is a positively weighted average of the values in (2.5), it follows that

$$\min[f(x_{j-1}), f(x_j), f(x_{j+1})] \le \bar{u}_j \le \max[f(x_{j-1}), f(x_j), f(x_{j+1})]. \tag{2.13}$$

Thus, since f is continuous, (2.12) possesses at least one root $\tilde{x}_j$ in the interval (x_{j-1}, x_{j+1}) and if f is monotonic the root is unique.

The required minimisers u and Π are obtained by solving (2.5) and (2.11) simultaneously. Combining these equations, the optimal grid points $\tilde{x}_j$ must satisfy

$$w_j^-(f(\tilde{x}_{j-1}) - f(\tilde{x}_j)) + w_j^+(f(\tilde{x}_j) - f(\tilde{x}_{j+1})) = 0 \quad (j = 1,\ldots,N). \tag{2.14}$$

2.2 A Double Iteration

Although a single iteration for the solution of (2.14) for the $\tilde{x}_j$ is readily devised, we shall prefer to set up a double iteration to repeatedly solve (2.5) and (2.11) in turn, so that the local part of the discrete norm, in the form (2.4) or (2.10), is decreased at each stage of the iteration so that it converges. In this double iteration the first step is to obtain u from (2.5);

the second step is to find a corrected grid from (2.11) for re-substitution into (2.5) to give a new u and so on.

The solution of (2.5) for u is immediate, but the solution of (2.12) for x requires an (inner) iteration of its own. Provided that f(x) is differentiable the Newton iteration,

$$x_j^{p+1} - x_j^p = \frac{\bar{u}_j - f(x_j^p)}{f'(x_j^p)} \tag{2.15}$$

$p = 1,2,\ldots)$ with $x_j^0 = x_j$, is possible but we could alternatively use bisection or a secant iteration (see below). Moreover, it is unnecessary to run this (inner) iteration to convergence since the main aim is to decrease the norm (2.10) within the outer iteration. Thus, since the change in the norm (2.10) as a result of the inner iteration from (2.10) and (2.12), is

$$(w_j^+ + w_j^-)[\{\bar{u}_j - f(x_j^p)\}^2 - \{\bar{u}_j - f(x_j)\}^2] \tag{2.16}$$

the inner iteration may be terminated as soon as

$$\left|\bar{u}_j - f(x_j^p\right| < \left|\bar{u}_j - f(x_j)\right|. \tag{2.17}$$

In particular, since

$$\begin{aligned} \bar{u}_j - f(x_j^{p+1}) &= \bar{u}_j - f(x_j^p) + (x_j^{p+1} - x_j^p)(-f'(\theta_p)) \\ &= \left[1 - \frac{f'(\theta_p)}{f'(x_j^p)}\right](\bar{u}_j - f(x_j^p)) \end{aligned} \tag{2.18}$$

where $\theta_p \in (x_j^p, x_j^{p+1})$, the termination condition (2.17) holds after one iteration if

$$\left|1 - \frac{f'(\theta_p)}{f'(x_j^p)}\right| < 1, \tag{2.19}$$

which is true provided that f' does not change sign or more than double its value locally within the interval.

The full algorithm is as follows:

1. Select a grid.
2. Generate u on the current grid from (2.5).
3. Use the iteration (2.15) (or some other inner iteration), terminated by (2.17), to obtain the new grid from (2.11).
4. If the norm is insufficiently small, return to step 2.

At convergence we see from writing (2.14) in the form

$$w_j^-\left(\frac{f(\tilde{x}_j)-f(\tilde{x}_{j-1})}{\tilde{x}_j-\tilde{x}_{j-1}}\right)(\tilde{x}_j-\tilde{x}_{j-1})=w_j^+\left(\frac{f(\tilde{x}_{j+1})-f(\tilde{x}_j)}{\tilde{x}_{j+1}-\tilde{x}_j}\right)(\tilde{x}_{j+1}-\tilde{x}_j) \qquad (2.20)$$

in that in the limit the weighted ratio of increments

$$w_j\left(\frac{f(\tilde{x}_{kR})-f(\tilde{x}_{kL})}{\tilde{x}_{kR}-\tilde{x}_{kL}}\right) \qquad (2.21)$$

is equidistributed on the grid.

2.3 An Order-preserving Iteration

We now consider an alternative inner iteration to (2.15) which has the desirable property that (apart from at certain points of extrema) the ordering of the partition Π is preserved. First, a secant-type version of (2.15) is generated by applying a modified Newton argument to (2.11), giving

$$x_j^{p+1}-x_j^p=\frac{w_j^-(u_j^- - f(x_j^p))+w_j^+(u_j^+ - f(x_j^p))}{w_j^-\left(\dfrac{u_j^- - f(x_j^p)}{x_G^- - x_j^p}\right)+w_j^+\left(\dfrac{u_j^+ - f(x_j^p)}{x_G^+ - x_j^p}\right)} \qquad (2.22)$$

where $x_G^- = x_{j-\frac{1}{2}}$, $x_G^+ = x_{j+\frac{1}{2}}$. Writing $u_j^- = f_G^-$, $u_j^+ = f_G^+$ (c.f. (2.5)), equation (2.22) can then be put in the form

$$x_j^{p+1} - x_j^p = \frac{(E_j^-)^p (x_G^- - x_j^p) + (E_j^-)^p (x_G^+ - x_j^p)}{(E_j^-)^p + (E_j^+)^p} \tag{2.23}$$

where

$$\left(E_j^{\pm}\right)^p = w_j^{\pm}\left(\frac{f_G^{\pm} - f(x_j^p)}{x_G^{\pm} - x_j^p}\right) = w_j^{\pm}\frac{\Delta^{\pm} f_{jG}^p}{\Delta^{\pm} x_G^p}, \tag{2.24}$$

say. (Note that the use of (2.5) is admissible here since the term $u_j^- - u_j^+$ in (2.10), being a difference of average values of f, does not contain $f(x_j)$.)

It may readily be deduced from (2.23) that, provided E_j^+ and E_j^- are of the same sign,

$$x_G^- < x_j^{p+1} < x_G^+ \tag{2.25}$$

and the partition therefore remains ordered during the iteration.

In many cases one step of the iteration (2.15) or (2.22) is sufficient to decrease the norm.

2.4 Equidistribution Properties

As we have already seen, in the limit an equidistribution function for the grid is $w\frac{\Delta f}{\Delta x}$. Consistently with (2.24) we write this function as

$$E = w\frac{\Delta f}{\Delta x}. \tag{2.26}$$

With the particular choice of weight $w = 1$, the equidistributed quantity is Δf, that is to say the grid can be constructed from equally spaced points on the ordinate axis, as in fig. 2. Monotonicity of f is required for the equidistribution in this case, since for more general functions convergence breaks down near extrema and chaotic behaviour is observed [3].

Other weights dependent on k are admissible, but weights dependent on u, x or function derivatives invalidate the norm-reduction argument based on (2.10). The double iteration, (2.5) and (2.10), may still converge, however, and again it is sufficient to run the inner iteration only as far as to satisfy the criterion (2.17). In practice it is found that convergence does occur for such weights and we mention two particular cases here.

The weight $w = \Delta x$ accentuates the contribution of large elements in the norm (2.1) which is then a trapezium rule approximation of the L_2 norm. The equidistributed quantity is $\Delta f \Delta x$, the area of a small box for which the arc length in an element is an approximate diagonal (see fig. 3(a)).

If f is differentiable and w is chosen such that

$$E = \frac{\Delta s}{\Delta x} \tag{2.27}$$

where

$$s = \int_0^x \left[1 + \{f'(\xi)\}^2\right]^{\frac{1}{2}} d\xi \tag{2.28}$$

is the arc length of the graph of f, the equidistributed quantity is Δs, as shown in fig. 3(b). The appropriate weight function is

$$w = \frac{\Delta s}{\Delta f} = \frac{\int_{x_{kL}}^{x_{kR}} [1 + \{f'(\xi)\}^2]^{\frac{1}{2}} d\xi}{f(x_{kR}) - f(x_{kL})}. \tag{2.29}$$

The function E of (2.27) may be approximated by

$$E = \left[1 + \left(\frac{\Delta f}{\Delta x}\right)^2\right]^{1/2}, \qquad (2.30)$$

although care is required in the use of (2.30) near extrema since the approximation may be significantly poor.

A similar approach to generating (2.27), (2.28) is to define the arc length function

$$s[f(x)] = \int_0^x [1 + \{f'(\xi)\}^2]^{1/2} d\xi \qquad (2.31)$$

which is always monotone, even though $f(x)$ may not be.

The piecewise constant approximation, $s[u]$ say, to (2.31) involves the norm

$$\| s[u] - s[f(x)] \|$$

whose minisation in the manner of this section will always lead to a converging iteration whose limiting grid equidistributes $\Delta s[f(x)]$ and therefore achieves the same result as (2.27), (2.28).

3. Two Dimensions

3.1 The Discrete Norm

Let $\Delta^0 = \{\Delta_k^0\}_{k=1}^M$ denote a triangulation of $\Omega = (0,1) \times (0,1)$. The closure is defined as $\bar{\Omega} = \bigcup_{k=1}^{M} \Delta_k^0$, where the Δ_k^0 are non-overlapping triangles such that no vertex of a triangle lies along the edge of another. Denote by T^M the set of all triangulations of Ω which have the same topological table as Δ^0, that is $\Delta \in \Upsilon^M$ if there is a one-to-one correspondence between Δ^0 and Δ which preserves the connections between vertices. For $\Delta \in \mathrm{Y}^M$ we define

$$D(\Delta) = \{v \in L^2(\Omega) | \, v|_\Delta = \text{constant}, \;\; k = 1,2,\ldots,M\}.$$

Now introduce the discrete norm $\|.\|$ with positive weight w given by

$$\|g\|^2 = \sum_{k=1}^{M} \sum_{v=1}^{3} w_k g(x_{kv}, y_{kv})^2 \tag{3.1}$$

where x_{kv}, y_{kv} are the coordinates of the $v'th$ vertex of Δ_k (see fig. 4(a).

Let $f \in C(\overline{\Omega})$. For each $\Delta \in \mathrm{T}^M$ we denote by $u = u(\Delta) \in D(\Delta)$ the projection of f onto $D(\Delta)$ in the above norm. Now write (3.1) in the form

$$\|g\|^2 = \sum_{k=1}^{M} \frac{1}{3} w_k \left\{ \left(\sum_{v=1}^{3} g_v \right)^2 + \sum_{\substack{\lambda=1 \\ \lambda > \mu}}^{3} \sum_{\mu=1}^{3} (g_\lambda - g_\mu)^2 \right\} \tag{3.2}$$

where $g_v = g(x_v, y_v)$ and λ, μ run over the same values of v. It follows that

$$\|v - f\|^2 = \sum_{k=1}^{M} \frac{1}{3} w_k \left\{ \left(3v - \sum_{v=1}^{3} f_{kv} \right)^2 + \sum_{\substack{\lambda=1 \\ \lambda > \mu}}^{3} \sum_{\mu=1}^{3} (f_{k\lambda} - f_{k\mu})^2 \right\}, \tag{3.3}$$

where $f_{kv} = f(x_{kv}, y_{kv})$, is minimised by the element u given by

$$u|_{\Delta_k} = \frac{1}{3} \sum_{v=1}^{3} f_{kv} = \overline{f}_k, \;\; \text{say} \tag{3.4}$$

(see fig. 4(a)).

The aim now is to find $\Delta \in \mathrm{T}^M$ such that

$$\|u(\Delta)-f\| \leq \|u(\tilde{\Delta})-f\| \qquad \forall \tilde{\Delta} \in y^M \qquad . \tag{3.5}$$

First rewrite (3.1) as

$$\|g\|^2 = \sum_{b=1}^{B} \sum_{e=1}^{ne(b)} w_b^e (g_b^e)^2 + \sum_{j=1}^{N} \sum_{e=1}^{ne(j)} w_j^e (g_b^e)^2 \tag{3.6}$$

where b is one of B boundary values and j is one of N internal vertices (with $N+B=M$). The index e runs over the number $ne(b)$ or $ne(j)$ of triangles with b or j as a common vertex, while

$$g_j^e = g_j \;|_{\Delta_e} \tag{3.7}$$

where Δ_e denotes the triangle with index e (see fig. 4(b)).

Now consider the identity

$$\sum_e w_j^e (g_b^e)^2 = \left\{ \left(\sum_e w_j^e g_j^e)^2 \right) + \sum_{\lambda > \mu} w_j^\lambda w_j^\mu (g_j^\lambda - g_j^\mu)^2 \right\} \Big/ \sum_e w_j^e \tag{3.8}$$

where λ, μ run over the same integers as e. The non-boundary terms of (3.6) then become

$$\sum_{j=1}^{N} \left[\left\{ \left(\sum_e w_j^e g_j^e \right)^2 + \sum_{\lambda > \mu} w_j^\lambda w_j^\mu (g_j^\lambda - g_j^\mu)^2 \right\} \Big/ \sum_e w_j^e \right] \tag{3.9}$$

and the corresponding terms in the norm of (3.3) are

$$\sum_{j=1}^{N} \left[\left\{ \left(\sum_e w_j^e (u_j^e - f_j) \right)^2 + \sum_{\lambda > \mu} w_j^\lambda w_j^\mu (u_j^\lambda - u_j^\mu)^2 \right\} \Big/ \sum_e w_j^e \right].$$

(All e summations, as well as λ, μ run from 1 to $ne(j)$).

Constraining the boundary notes to remain fixed for the moment, it follows that, for a given piecewise constant u, the norm of (3.3) is minimised by the triangulation Δ with vertices satisfying

$$\sum_e w_j^e (u_j^e - f_j) = 0 \tag{3.11}$$

or

$$f(x_j, y_j) = \sum_e w_j^e u_j^e \Big/ \sum_e w_j^e = \overline{u}_j \quad \text{say} \tag{3.12}$$

(c.f.(2.12)). A similar argument may be applied to the boundary terms in (3.4) with the boundary vertices constrained in some way to remain on the boundary.

Since the right hand side of (3.12) is a positively weighted average of (3.4), it follows that

$$\min_v f_{jv} \leq \overline{u}_j \leq \max_v f_{jv}, \tag{3.13}$$

where the suffix jv runs over all the vertices of the triangles which have j as a common vertex (see fig. 5). Hence, since $f(x,y)$ is continuous, (3.12) possesses a solution on at least one "spoke" joining the vertex j to one of the outer vertices in fig. 5. More generally, solutions of (3.12) will lie on a contour of $f(x,y)$, at least part of which is contained within the local patch of triangles in fig. 5.

The required minimisers u and Π are obtained by solving (3.4) and (3.12) simultaneously. The resulting solution therefore satisfies

$$\sum_e w_j^e (\overline{f}_e - f_j) = 0 \tag{3.14}$$

where

$$\overline{f}_e = \frac{1}{3}\sum_{\nu=1}^{3} f(x_{e\nu}, y_{e\nu}). \tag{3.15}$$

3.2 A Double Iteration

As an alternative to solving (3.14) directly, we may find a solution of (3.4) and (3.12), as in one dimension, by setting up a double iteration, each step of which reduces the norm of the error. The only new factor is that in higher dimensions the solution of (3.12) for (x_j, y_j) is not unique. We shall need an appropriate (inner) iteration in order to extract a solution although, as in one dimension, the inner iteration need only be run until the norm is decreased. Since the change in the norm (3.10) is

$$\sum_e w_j^e \left[\left(\overline{u}_j - f(x^p, y_j^p)\right)^2 - \left(\overline{u}_j - f(x_j, y_j)\right)^2 \right] \tag{3.16}$$

(c.f. (2.25)), it is again sufficient to use

$$\left| f(x_j^p, y_j^p) - \overline{u}_j \right| < \left| f(x_j, y_j) - \overline{u}_j \right| \tag{3.17}$$

as a stopping criterion.

The usual Newton argument on (3.12) gives

$$0 = \overline{u}_j - f(x_j^{p+1}, y_j^{p+1}) = \overline{u}_j - f(x_j^p, y^p) - (x_j^{p+1} - x_j^p, y_j^{p+1} - y_j^p).\underline{\nabla} f_j^p . \tag{3.18}$$

To minimise the possibility of mesh tangling we shall choose the displacement with smallest modulus, giving

$$(x_j^{p+1} - x_j^p, y_j^{p+1} - y_j^p) = \left(\frac{\{\overline{u}_j - f(x_j, y_j)\}}{|\underline{\nabla} f|_j} \hat{\underline{\phi}}_j \right)^p \tag{3.19}$$

where $\hat{\underline{\phi}}_j$ is a unit vector in the direction of $\underline{\nabla} f_j$.

3.3 A Local Iteration

As in one dimension, a secant version of (3.19) may be constructed from a modified version of (3.18), namely,

$$0 = \sum w_j^e \{u_j^e - f(x_j^p, y_j^p)\} - (x_j^{p+1} - x_j^p, y_j^{p+1} - y_j^p).\left(x_j^p \sum w_j^e \underline{\nabla} \tilde{f}^e\right)^p \qquad (3.20)$$

where $\tilde{f}$ is the linear interpolant of f. Again, choosing the displacement with smallest modulus, (3.20) leads to

$$(x_j^{p+1} - x_j^p, y_j^{p+1} - y_j^p) = \left(\frac{(\sum w_j^e \{u_j^e - f(x_j, y_j)\})}{\sum w_j^e |\underline{\nabla} \tilde{f}|^e} \tilde{\underline{\phi}}_j \right)^p \qquad (3.21)$$

where $\tilde{\underline{\phi}}_j$ is a unit vector in the direction of $\sum w_j^e (\underline{\nabla} \tilde{f})^e$. (All summations are again from $e = 1$ to $e = ne(j)$.)

From (3.12) and (3.4)

$$\sum w_j^e u_j^e = \sum w_j^e \bar{u}_j = \sum w_j^e \tilde{f}_G^e, \text{ say} \qquad (3.22)$$

so that the numerator on the right hand side of (3.21) becomes

$$\left(\sum w_j^e \{\tilde{f}_G^e - f(x_j, y_j)\}\right) \tilde{\underline{\phi}}_j \qquad (3.23)$$

evaluated at the p'th iteration. It is this quantity which vanishes in the convergent limit and corresponds to the equidistribution property in 1-D.

Since

$$(\tilde{f}_G^e - f(x_j, y_j) = (x_G - x_j, y_G - y_j).\underline{\nabla}\tilde{f}^e = \underline{r}_{jG}.\underline{\nabla}\tilde{f}^e, \text{ say,} \qquad (3.24)$$

where $\tilde{f}$ is the linear interpolant of f.

Then (3.23) may be written

$$\left(\sum w_j^e \underline{r}_{jG}.\underline{\nabla}\tilde{f}^e\right)\underline{\tilde{\phi}}_j. \qquad (3.25)$$

Although we have used (3.4), this is admissible as in the argument following (2.2).

The iteration step (3.21) then becomes

$$(x_j^{p+1} - x_j^p, y_j^{p+1} - y_j^p) = \left(\frac{(\Sigma w_j^e \underline{\nabla}\tilde{f}^e.\underline{r}_{jG}^e)}{\Sigma w_j^e \left|\underline{\nabla}\tilde{f}^e\right|}\underline{\tilde{\phi}}_j\right)^p \qquad (3.26)$$

$$= \left(\frac{\Sigma w_j^e \left|\underline{\nabla}\tilde{f}^e\right| \underline{t}_{jG}^e}{\Sigma w_j^e \left|\underline{\nabla}\tilde{f}^e\right|}\right)^p \qquad (3.27)$$

where $\underline{t}_{jG}^e$ is the projection of $\underline{r}_{jG}$ into $\underline{\tilde{\phi}}_j$ as shown in fig.6.

It is clear from (3.27) that the displacement of the node j in the direction $\underline{\tilde{\phi}}_j$ is contained within the degenerate polygon which has $\underline{t}^e_{jG}$ as vertices. In the limit the "equidistribution" property

$$\sum w^e_j \left|\underline{\nabla} \tilde{f}^e\right| \underline{t}^e_{jG} = 0 \tag{3.28}$$

holds.

Unlike in one dimension, this property does not necessarily preclude mesh tangling, as the particular example in fig. 7 shows. It is therefore necessary to add a limiting factor to (3.27). A sufficient condition is that the magnitude of the displacement should not be greater than half the maximum triangle height of all the triangles in the patch of fig. 5.

As in one dimension, when the weights are allowed to depend only on e the norm-decreasing property still holds but if they are allowed to depend on u, x or y the property may be lost. Nevertheless the iteration may still converge and in particular the choices

(a) w^e = area of element e (3.29)

and

(b) $$w^e = \left\{1 + \left(\left|\underline{\nabla} \tilde{f}^e\right|\right)^2\right\}^{½} \Big/ \left|\underline{\nabla} \tilde{f}^e\right| \tag{3.30}$$

(the latter corresponding to the choice (2.30) in one dimension) allows extra weight to be put on the surface area of the solution.

The "equidistribution" property (3.28) is comparable to (2.20). We may also write it as

$$\sum E_j^e \underline{t}_{jG}^e = 0 \tag{3.31}$$

where

$$E_j^e = w_j^e \left| \nabla \tilde{f}^e \right| . \tag{3.32}$$

With this definition of E, the iteration (3.27) may be written

$$(x_j^{p+1} - x_j^p, y_j^{p+1} - y_j^p) = \frac{\Sigma E_j^e \underline{t}_{jG}^e}{\Sigma E_j^e} . \tag{3.33}$$

The full algorithm may be stated as follows:

1. Select a grid

2. Use (3.10) to generate values of $\bar{u}_j$ on the current grid.

3. Use the iteration (3.19) (or some other inner iteration such as (3.27) or (3.31)), terminated by (3.17), to obtain new values of x_j, y_j.

4. If the reduction in the norm is insufficiently small, return to step 2.

4. An Averaging Procedure

There is a striking similarity between the displacement (3.27) or (3.33) and the displacement

$$\delta \underline{r}_j = \frac{\Sigma w_j^e \left|\underline{\nabla} \tilde{f}^e\right| \underline{r}_{jG}^e}{\Sigma w_j^e \left|\underline{\nabla} \tilde{f}^e\right|} = \frac{\Sigma E_j^e \underline{r}_{jG}^e}{\Sigma E_j^e} \tag{4.1}$$

(c.f. fig. 6) often used to relocate nodes in grid generation work, in that the component of (4.1) in the direction $\underline{\tilde{\phi}}_j$ is precisely (3.27). Indeed, we may regard (4.1) as providing not only the correct node displacement in the $\underline{\tilde{\phi}}_j$ direction but also a convenient displacement in the orthogonal direction which serves to smooth out inter-nodal irregularities which may occur as a result of corresponding irregularities in $\underline{\tilde{\phi}}$.

It is clear that a single iteration (4.1) can be used as an alternative to (3.27) in order to decrease the norm. The displacement is then confined to the non-degenerate polygon with $\underline{r}_{jG}^e$ as vertices: the anti-tangling constraint will still be required, in general.

The semi-heuristic step (4.1) gives a different "equidistribution" property in the limit, namely,

$$\sum w_j^e \left|\underline{\nabla} \tilde{f}^e\right| \underline{r}_{jG}^e = \sum E_j^e \underline{r}_{jG}^e = 0 \tag{4.2}$$

with E_j^e defined by (3.32) (c.f.(3.30)) which determines (x_j, y_j) as the centre of mass of particles of mass $w_j^e \left|\underline{\nabla} \tilde{f}\right|^e$ at the centroids of surrounding triangles.

Another way of interpreting (4.2) is to regard it as a discretisation of the differential operator

$$\underset{\sim}{\nabla}(w|\underline{\nabla}\tilde{f}|\underset{\sim}{\nabla}\underline{r}) = \underset{\sim}{\nabla}(E\underset{\sim}{\nabla}\underline{r}) = 0, \tag{4.3}$$

where $\underset{\sim}{\nabla}$ denotes $\left(\frac{\partial}{\partial\xi}, \frac{\partial}{\partial\eta}\right)$. Here (ξ, η) denotes a fixed reference grid and E is a "diffusion coefficient". Then the iteration (4.1) is a discretisation of

$$\delta\underline{r} = \theta\underset{\sim}{\nabla}(w|\underline{\nabla}\tilde{f}|\underset{\sim}{\nabla}\underline{r}) = \theta\underset{\sim}{\nabla}(E\underset{\sim}{\nabla}\underline{r}) \tag{4.4}$$

where θ is a relaxation parameter.

We may also regard (4.3) as a minimisation, that of

$$\min_{\underline{r}} \int w|\underline{\nabla}\tilde{f}|(\underset{\sim}{\nabla}\underline{r})^2 d\underline{\xi} \tag{4.5}$$

or

$$\min_{\underline{r}} \int E(\underset{\sim}{\nabla}\underline{r})^2 d\underline{\xi}. \tag{4.6}$$

5. Generalisations

The algorithm described in section 3 is not restricted to triangles. By replacing the upper suffix 3 in (3.1) by 4,5 etc. we may extend the algorithm to quadrilaterals, pentagons, etc. The forms of (3.1) require for a general N-sided polygon are

$$\|g\|^2 = \sum_{k=1}^{M} \frac{1}{N} w_k \left\{ \left(\sum_{\nu=1}^{N} g_\nu \right)^2 + \sum_{\lambda=1}^{N} \sum_{\mu=1}^{N} (g_\lambda - g_\mu)^2 \right\} \tag{5.1}$$

in place of (3.2), and (3.8) as it stands, where e runs over the number of polygons having j as a common vertex.

The piecewise constant function u in (3.4) is then given by

$$u\Big|_{\Delta k} = \frac{1}{N} \sum_{\nu=1}^{N} f_{k\nu} \tag{5.2}$$

while the formula for x_j, y_j in (3.11), (3.12) still stands. The iteration (3.24) can be used and the stopping criterion (3.17) is still valid. The only difficulty is the lack of a unique piecewise linear interpolant $\tilde{f}$ which prevents the step (3.24) being carried out. Thus the formula (3.27) holds only in an approximate sense and its similarity with (3.31) is partially lost.

On the other hand, the extension to higher dimensions using tetrahedrons goes through without difficulty. Here Δ_k denotes a tetrahedron and the corresponding forms of (3.1) required are (3.3) with 3 replaced by 4 and (3.10), with $ne(j)$ being the number of tetrahedra having j as a common vertex.

6. Demonstrations

We show results for four functions, two in one dimension and two in two dimensions. The one-dimensional functions are

(a) $\tanh\ 32(x - 0.5)$

(b) $10e - 10x \ + 20/\{1 + 400(x-0.7)2\}$

on $[0,1]$, starting from an equally spaced grid. Case (a) was run for 100 steps and (b) for 400 steps. Figs 8 and 9 show case (a) with weights $w = 1$ and (2.31), respectively. Fig. 10 shows case (b) with weight (2.31).

The two-dimensional functions are

(c) $\tanh\ 32(x + y - 0.5)$

(d) $\tanh 32(x^2 + y^2 - 0.25)$

on $[0,1] \times [0,1]$, starting from a set of subdivided quadrilaterals, as in fig. 11. Case (c) was run for 100 steps and (d) for 40 steps. The final grids and profiles for $w = 1$ are shown in fig 12 and those for w given by (3.29) are shown in fig 13.

In addition, the corresponding grids and functions for the grid adapter given in (4.1) are shown in figs. 14 and 15.

7. Conclusions and Discussions

In this report we have described algorithms for finding best approximation to continuous functions by piecewise constant approximations with variable nodes, using the discrete norm (2.1). The algorithms take the form of a double iteration, one for the solution and one for the nodes which guarantee norm reduction. The node step itself involves an (inner) iteration which however can usually be restricted to one or two steps to give reduction of the norm. There is a link between one step of the inner iteration and averaging procedures often used in grid adaptation.

The norm-reduction property holds true when weighted by a term which involves neither the solution nor the grid. If more general weights are used the performance is still good although there is no proof of norm-reduction.

The resulting grids have equidistribution properties in one dimension and also have generalisations of this idea in higher dimensions which involve the solution of discretisations of nonlinear elliptic equations.

One problem with the algorithm when the weight is unity is the possibility of E changing sign in (2.23) near to extrema. There are two possible remedies. One is to fix the node at or near an extremum by replacing the r.h.s. of (2.23) by zero when $E_j^- E_j^+ \leq 0$. This has been done in the demonstration (b) in one dimension (fig. 9). The alternative remedy is to replace E everywhere by $|E|$ (as has effectively been done in two dimensions, c.f. (3.27)). However, there is still a potential problem when all the $|E|$'s in the vicinity of a node are small, in that the ratio in (3.27), for example, is of two vanishingly small numbers. A solution to this problem is to replace $|E|$ by a small non-zero constant value when $|E|$ is small. A constant E will have the effect of smoothing the grid since the corresponding equidistributed quantity is then x itself.

Finally, in the two-dimensional case, there is the possibility of edge-swapping, i.e. the interchanging of the diagonal of a quadrilateral made up of a pair of adjacent triangles if the norm is thus reduced. This also introduces, for the first time, a change in the topology of the grid if that so reduces the norm.

8. References

1. **Baines, M.J.,** Algorithms for Optimal Discontinuous Piecewise Linear and Constant L_2 Fits to Continuous Functions with Adjustable Nodes in One and Two Dimensions. Math. Comp. 62,645-669 (1994).

2. **Tourigny, Y. & Baines, M.J.,** Analysis of an Algorithm Iterative for Generating Locally Optimal Meshes for L_2 Approximation by Discontinuous Piecewise Polynomials (submitted to Math. Comp.) (1995).

3. **Sweby P.K.,** Private Communication, Department of Mathematics, University of Reading, (1994).

4. **Lawson, C.L.** Software for C^1 Interpolation. In Mathematical Software III (Academic Press, New York) J.R. Rice (ed.))pp.161-194 (1977).

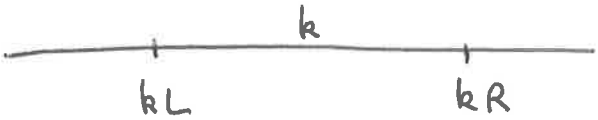

Fig. 1(a)

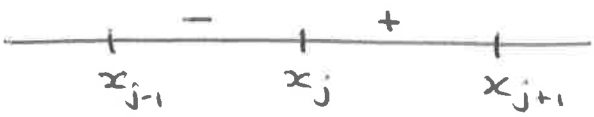

Fig. 1(b)

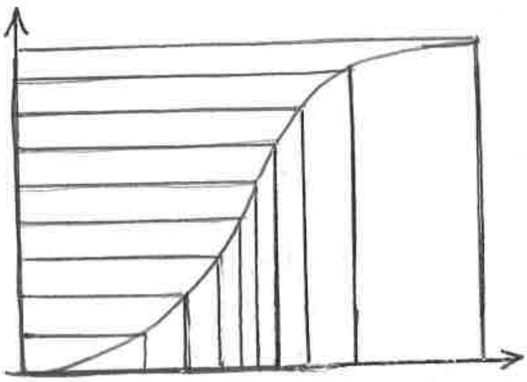

Fig. 2

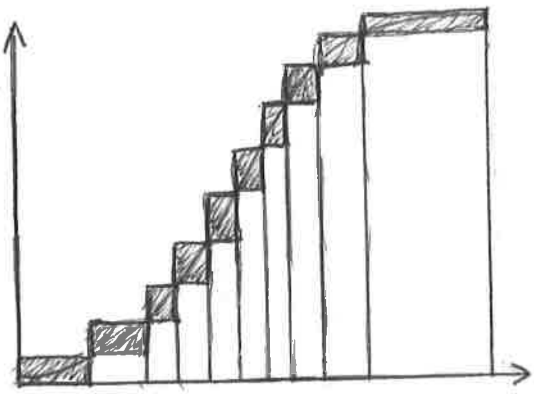

Fig. 3(a)

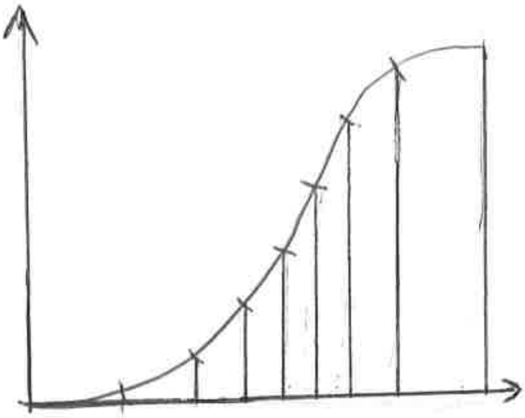

Fig. 3(b)

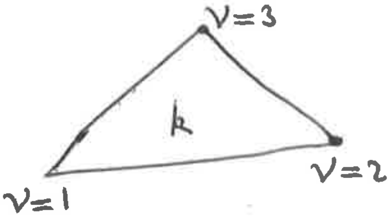

Fig. 4(a)

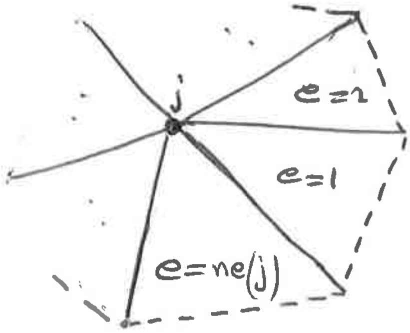

Fig. 4(b)

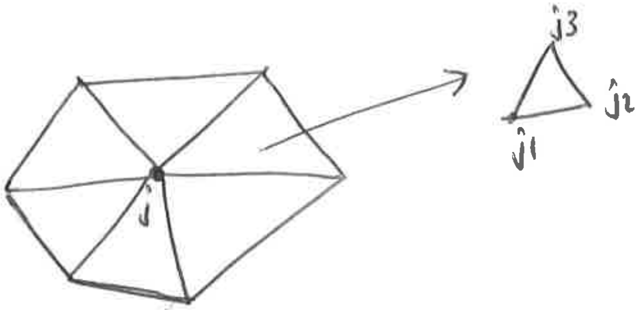

Fig. 5

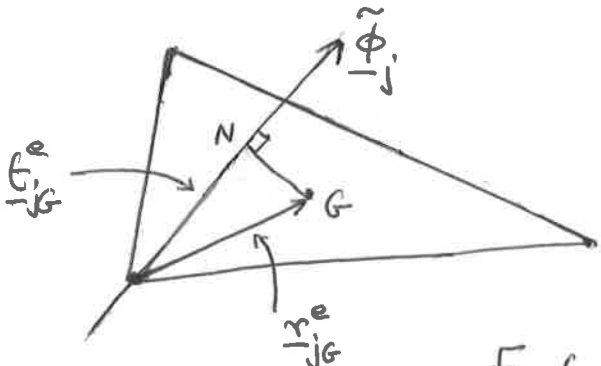

Fig. 6.

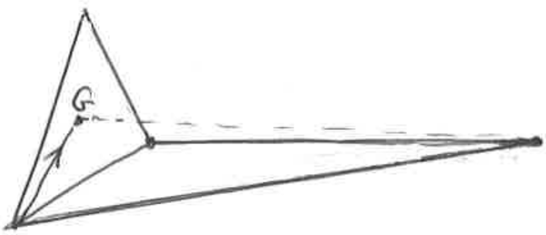

Fig. 7

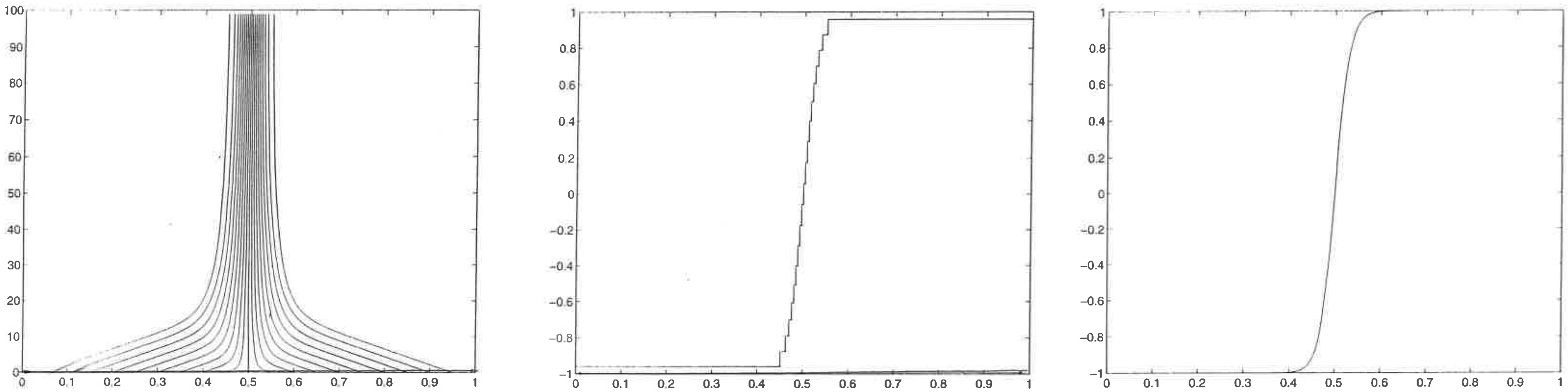

Fig. 8. Trajectories, best fit, and function for problem (a) with $w=1$

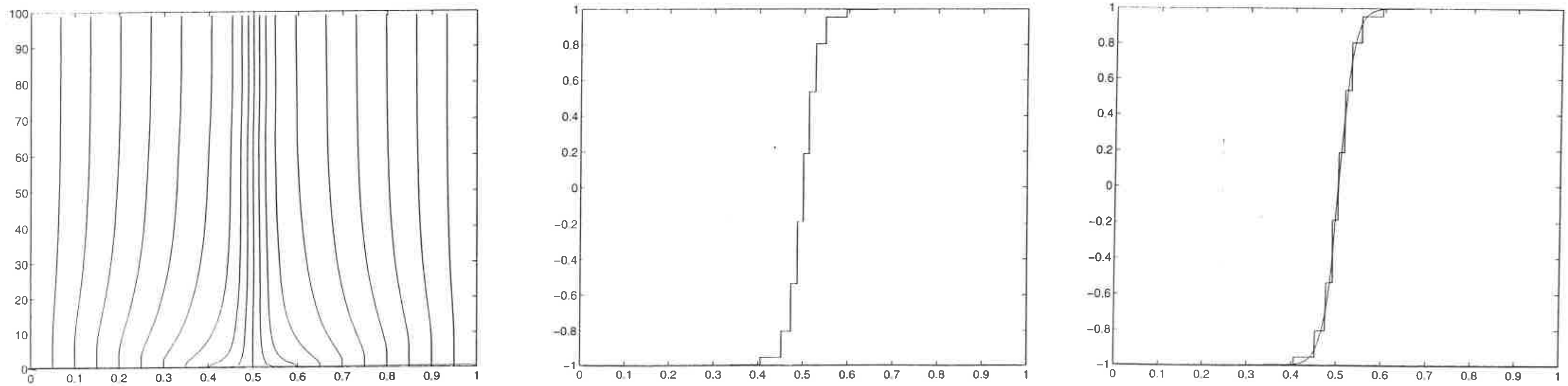

Fig. 9. Trajectories, best fit, and comparison with the function for problem (a) with weight given by (2.31).

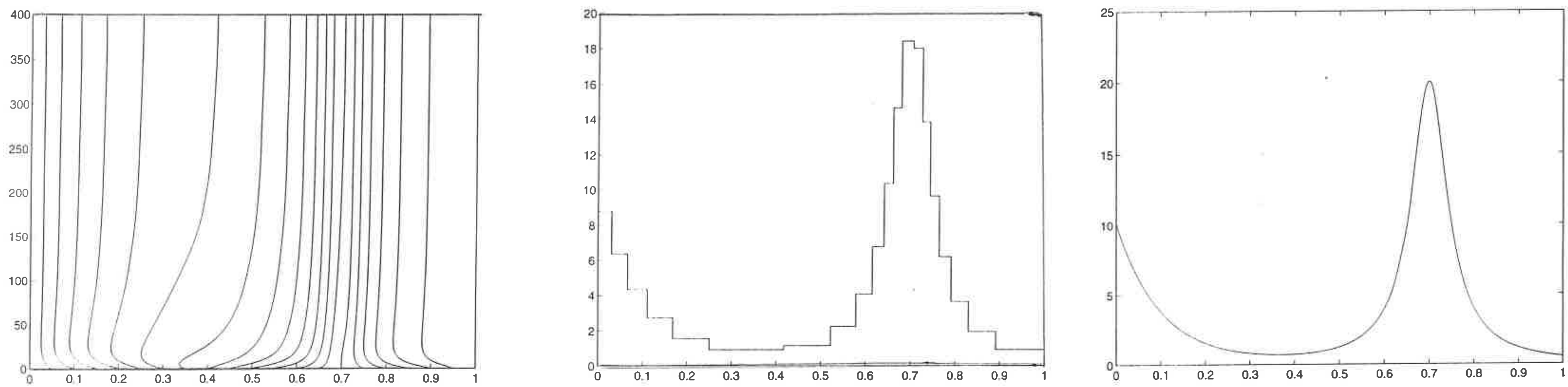

Fig. 10. Trajectories, best fit, and function for problem (b) with weight given by (2.31)

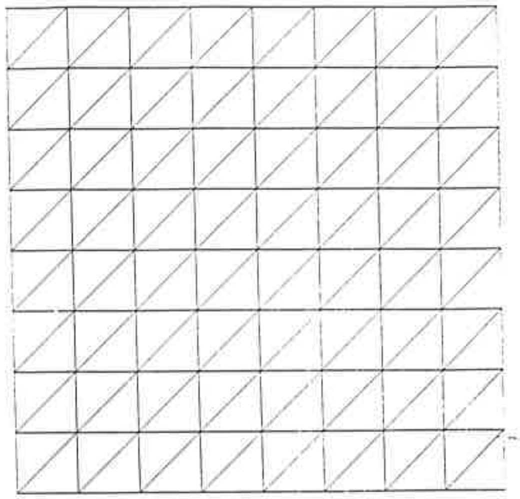

Fig. 11 Initial Grid

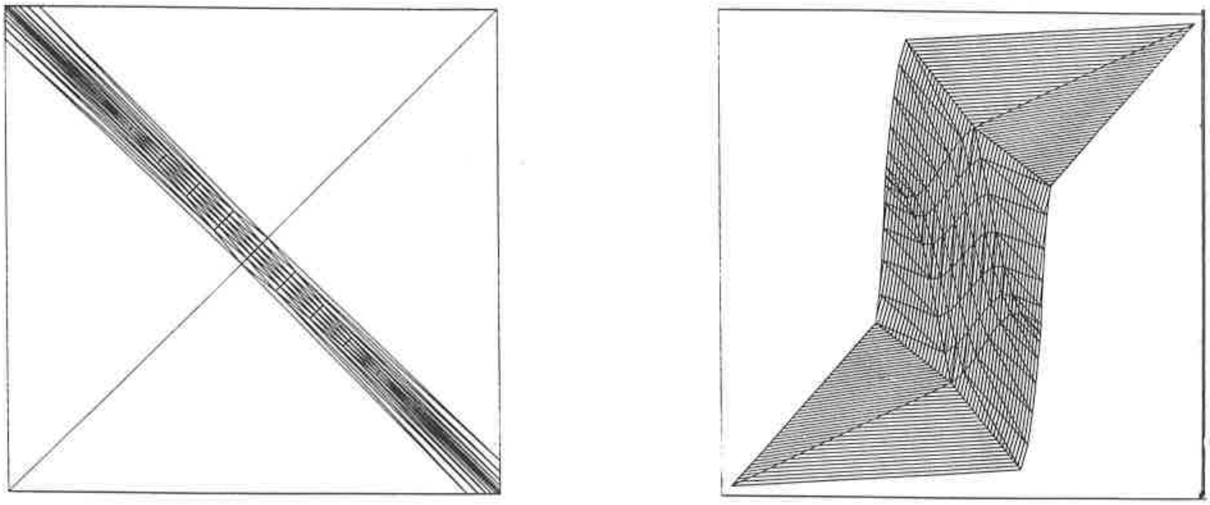

(c)

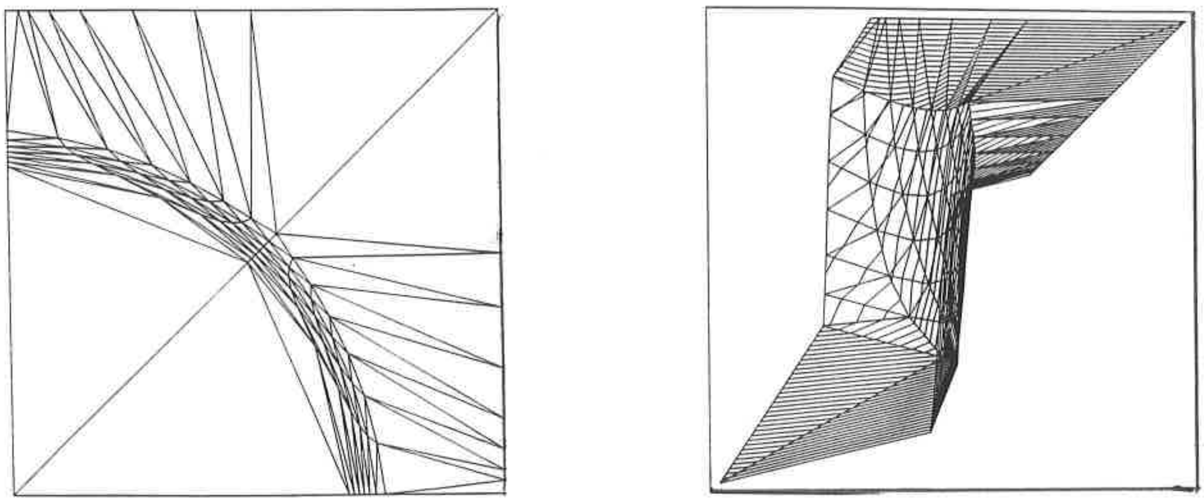

(d)

Fig. 12. Final grid and profile for functions (c) and (d) with $w = 1$.

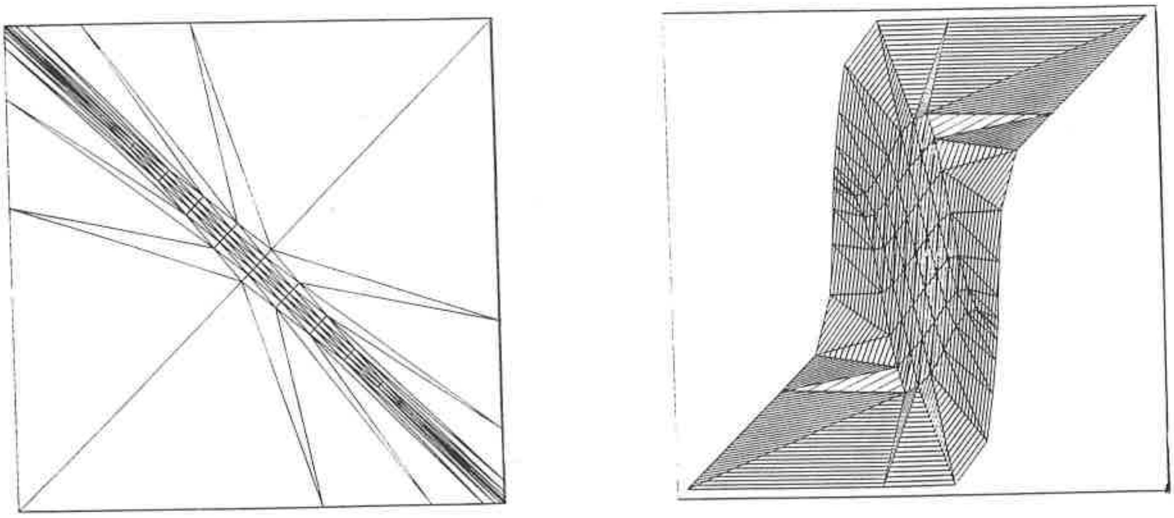

(c)

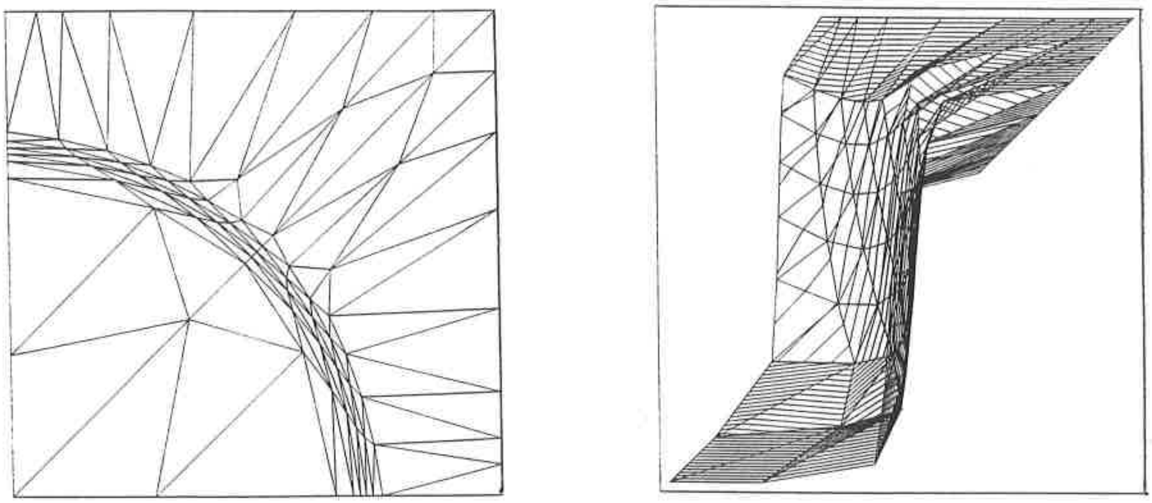

(d)

Fig. 13. Final grids and profiles for functions (c) and (d) for weight given by (3.24).

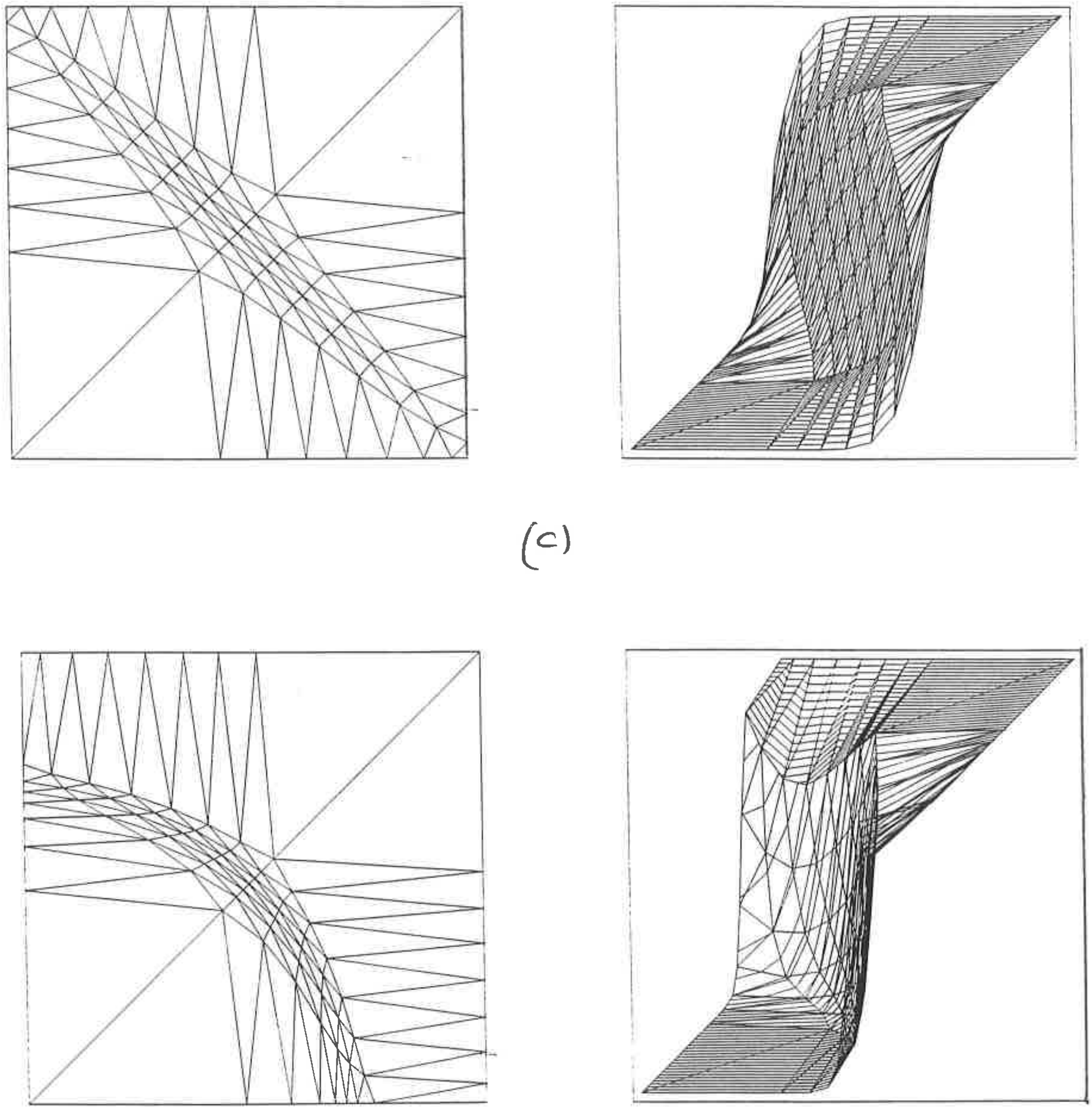

Fig. 14. Final grids and profiles for functions (c) and (d) for the grid adapter of (4.1) with weight = 1

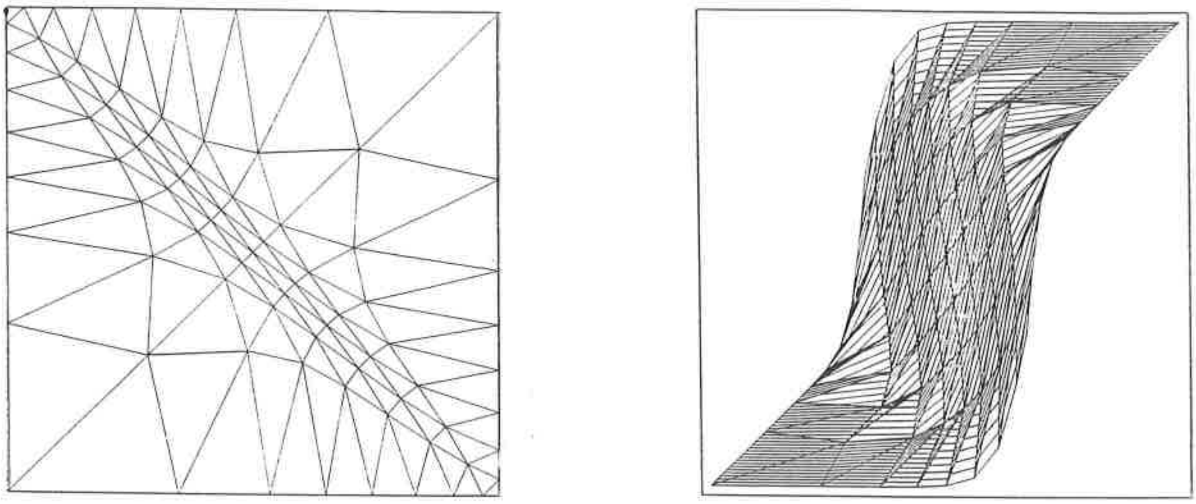

(c)

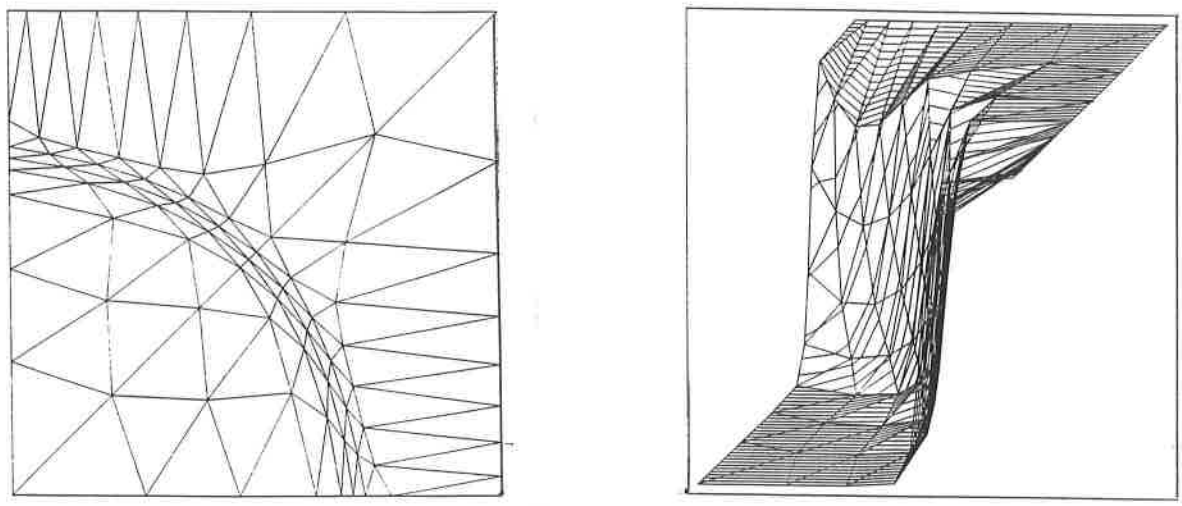

(d)

Fig. 15 Final grids and profiles for functions (c) and (d) for the grid adapter of (4.1) with weight given by (3.29).